Catalysis Today 441 (2024) 114867

Contents lists available at ScienceDirect

Catalysis Today

journal homepage: www.elsevier.com/locate/cattod

The importance of Pd carbide formation for reactions with ethene and other organic molecules

M. Bowker [a,b,*]

[a] Max Planck-Cardiff Centre on the Fundamentals of Heterogeneous Catalysis FUNCAT, Cardiff Catalysis Institute, School of Chemistry, Cardiff University, Maindy Road, Cardiff, CF OX11 0FA, UK
[b] UK Catalysis Hub, RCAH, Rutherford Appleton Lab, Harwell, Oxfordshire OX11 0FA, UK

ARTICLE INFO

Keywords:
Palladium
Palladium carbide
Ethene
Ethene disproportionation
Acetaldehyde
Decarbonylation

ABSTRACT

The reactions of a range of unsaturated hydrocarbons and oxygenated organic molecules with pure Pd surfaces can result in the carbidisation of the bulk of the metal, even though Pd is not usually recognised as a carbide-forming material. This can have important implications for catalysis by Pd. In this personal review it is shown that for the case of ethene, such bulk carbidisation is very fast above about 400 K. Adsorption and reaction with both pure single crystal Pd and supported nanoparticulate Pd is reported. For the former every ethene molecule has a 70 % probability per collision with the surface of dehydrogenating and depositing C into the metal. At low temperature (400 K) this accumulates near the surface, while at higher temperatures the C dissolves in the bulk and is reduced in the surface region. It can be retrieved by treatment in oxygen. For the nanoparticulate metal, the bulk is saturated very quickly with C, ultimately making a Pd_4C-like material. During this time a disproportionation reaction occurs in which methane only evolves into the gas phase and C is deposited in the Pd. Once the bulk is saturated with C, then reaction with ethene stops. It is shown that similar carbidisation also takes place with acetaldehyde.

1. Introduction

We are familiar with the reactivity dependence of elements in the transition series, highlighted as the 'Volcano Principle" [1], or Sabatier Principle [2] and described in many textbooks [3–7]. Here it is stated that, depending on which reactions are concerned, there is generally a maximum in reaction rate in the late transition series. For example, for ammonia synthesis Fe is the best practical catalyst for a variety of reasons, although Os and Ru could be better in some respects [8,9]. For fuel refining operations, such as naphtha reforming [10], Pt is considered the best material, while for many fine chemicals and pharmaceutical hydrogenation reactions Pd is favoured [11]. For the hydrogenation of CO and/or CO_2 to methanol, Cu is the best material [12]. However, it is very rarely the case that the pure element is the active phase, and here I am not considering the use of an inert support material which is usually applied to increase active surface area and stability. So, to illustrate this point, and returning to the reactions above, Fe alone is not so active for ammonia synthesis, but is used in conjunction with alkalis, generally K, which is present at the surface, to lower the barrier to the reaction [8, 13–15]. For naphtha reforming Pt is used in conjunction with Sn, and indeed is present as an alloy [16], while for methanol synthesis it appears that Cu has to be present in conjunction with a reducible support, especially ZnO, to give the best performance, and some authors propose that it is some form of a surface [17–19] or bulk [20] Zn alloy of Cu that is actually the active species.

So, the 'Volcano plot' really needs to be rewritten for elements in conjunction with activity/selectivity moderators for particular types of well-known reactions. The volcano plot is usually presented in the form of specific rate against position in the periodic table. But a variety of factors can affect the maximum in this rate. For instance, for a single metal surface energy is really the driver, so that the rate increases with a decrease in surface atom coordination (surface energy), that is the rate varies depending upon the surface plane exposed on the nanoparticle. But the addition of electronegative or electropositive elements has an effect on the surface electron density and its distribution at the atomic scale, which then affects rate and the position of the maximum in the transition series.

In this paper I concentrate on the behaviour of Pd, which appears to

* Corresponding author at: Max Planck-Cardiff Centre on the Fundamentals of Heterogeneous Catalysis FUNCAT, Cardiff Catalysis Institute, School of Chemistry, Cardiff University, Maindy Road, Cardiff, CF OX11 0FA, UK.
E-mail address: bowkerm@cardiff.ac.uk.

https://doi.org/10.1016/j.cattod.2024.114867
Received 25 April 2024; Received in revised form 20 May 2024; Accepted 31 May 2024
Available online 1 June 2024

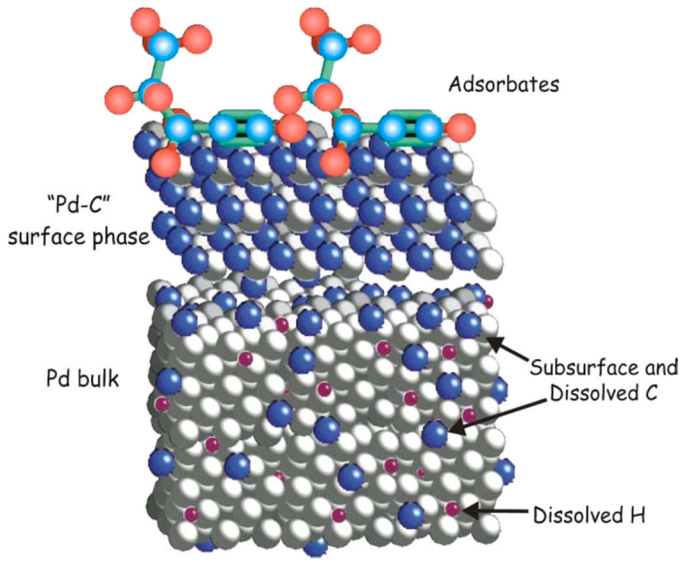

Fig. 1. A model of a Pd surface during pentyne hydrogenation, from the work of Teschner et al. [23].

have rather unusual properties compared with other elements around it, in that it can absorb many element types in a relatively facile manner during reactions, as described below.

The focus here, then, is C incorporation into/onto Pd, something which the Glasgow group has been involved with for a number of years [21–27]. In 1990 Thomson and Webb suggested that the direct transfer of hydrogen to alkenes does not happen, but rather there is migration of hydrogen from C species on the surface to the incoming alkene. [21] David Jackson, in whose honour this Glasgow meeting was held, continued this work, focussing on Pd as a hydrogenation catalyst [22–24] and including work with Geoff Webb. With Teschner et al., he showed that during selective pentyne hydrogenation both surface and bulk C were present on/in the Pd nanoparticles used (Fig. 1). They proposed that, rather than being a H-transfer agent, the C plays the role of moderating the activity of hydrogen to enable the partial hydrogenation to the pentyne to take place selectively.

Prior to this latter work Bowker et al. reported on the significance of C in the surface and bulk of Pd in relation to a totally different reaction, namely the acetoxylation of ethene to vinyl acetate [28–32]. They then went on to carry out an extensive study of the nature of C deposition and diffusion into Pd from ethene adsorption on single crystals [33,34] and catalysts [35], and this is described below.

More recently, Bugaev et al. [36–39] have published several papers on the subject of Pd carbidisation, using a variety of techniques and especially XAS, focussing on carbide formation during ethene adsorption and hydrogenation. They showed that during in situ hydrogenation of ethene that the Pd catalysts (Pd/C) carbidises, even in an excess of H_2 and even at temperatures as low as 350 K, and that the carbide is important for catalytic activity [36]. They also showed that the carbide is formed quicker under acetylene treatment compared with ethylene [37].

A number of theoretical approaches have been used to understand the carbidisation process. He and Wu calculated the dissolution characteristics of C using calculations on a slab of Pd using CMC methods, finding a variety of pathways for C to incorporate into the subsurface layers of Pd, depending on which surface geometry was used [40]. The barriers to diffusion into the bulk of the slab were calculated to be ~1.5 eV, or ~ 140 kJ/mol. They calculated a number of C concentrations including very high ones, with high binding energies of C in the bulk for all. Calculations using DFT using a small nanoparticle geometry by Kordatos et al. [41] found similarities and differences with the previous work of He and Wu. Activation barriers into immediate subsurface states on the very small nanoparticles (diameter ~ 1 nm) varied from ~ 30–150 kJ/mol, depending on which surface plane the carbon atom begins. Surprisingly the barrier to subsurface diffusion from the close-packed (111) plane was much easier than through the (100) plane.

This paper concerns the unusual nature of Pd and its ability to act as an 'atomic sponge' for carbon in a relatively facile way, but also for

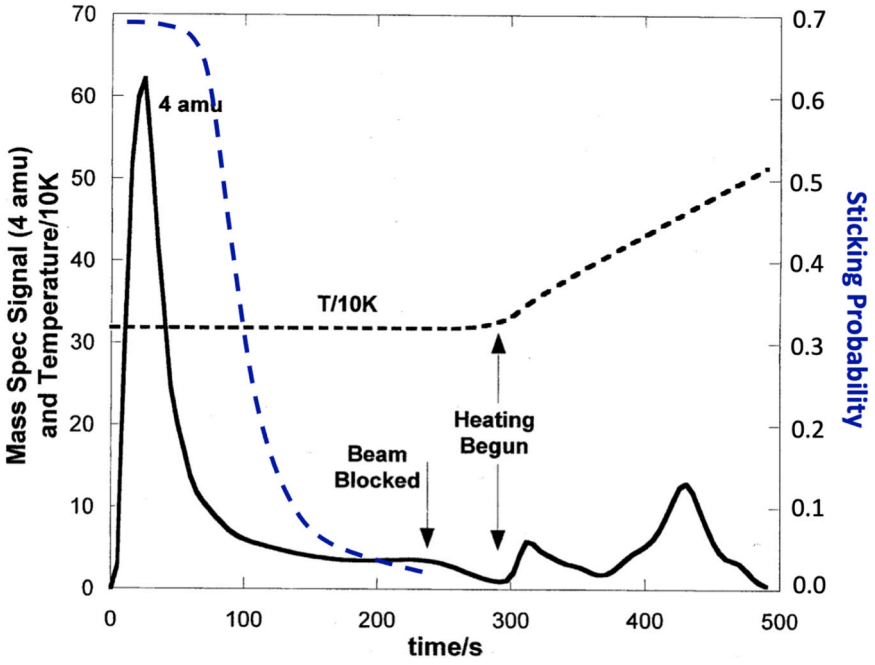

Fig. 2. Molecular beam reactor measurements of the adsorption of fully deuterated ethene on a pure Pd surface, Pd(110) at 318 K. This shows the sticking probability (blue dashed line), equivalent to the adsorption probability of stable species at this temperature, and the evolution of deuterium during this adsorption. The beam of ethene is blocked after 240 seconds, after which the deuterium evolution declines, but then a temperature ramp is applied, during which some more D_2 evolves, due to the decomposition of remaining carbonaceous species. Amended figure from Bowker et al. [28,31].

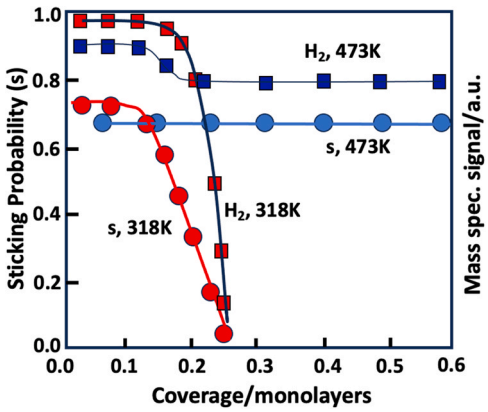

Fig. 3. Contrasting the reactivity of ethene with pure Pd(110) at low temperature and high temperature. At the low temperature, sticking finishes after adsorption of about 0.25 monolayers of ethene, during which hydrogen evolves into the gas phase, but stops when adsorption stops, and the surface is covered and blocked by adsorbed species. However, at 473 K, there is steady state sticking at 0.67 probability, with continuous hydrogen evolution. Indeed, this evolution appears to go on indefinitely, for the longest experiment it still continues even after 20 monolayers equivalent of ethene have adsorbed. Amended figure from Bowker et al. [33].

other elements, enabling the mutability of its catalytic properties by such incorporation.

2. Results and discussion

2.1. Carbidisation of Pd on pure crystals and on supported catalysts

Carbidisation of bulk single crystals. Pure Pd can be classed as a dehydrogenator of organic molecules. An example of this for a well-defined surface of Pd is given in Fig. 2, where ethene is adsorbed from a molecular beam of pure ethene onto a Pd(110) surface [28–30]; the similar behaviour of a range of other molecules is reported further below. Here it can be seen that ethene is dehydrogenated by the surface during adsorption at 318 K and at the end of this period the adsorption probability has dropped to zero, but it leaves a dehydrogenated intermediate, thought to be C_2H, on the surface [28]. This stoichiometry derives from the ratio of D_2 evolved during adsorption of C_2D_4 at ambient temperature, which removes most of the D in the molecule, to that evolved at higher temperature, combined with the IRAS results of Nishijima et al. [42,43] and the more recent DRIFTS/XAS results of Usoltsev et al. [39]

Fig. 3 contrasts adsorption at 318 K temperature with that at 473 K. For the former adsorption stops after 0.25 monolayers of ethene have adsorbed, whereas at the higher temperature adsorption appears to continue at a high rate indefinitely (with a continuing adsorption probability 0.67) [28]. The only product is hydrogen into the gas phase, so C is left on the crystal at 473 K. I would imagine, however, if that were the case, that adsorption would be blocked after a while, but at 473 K it is not, and this implies that C diffuses away from the surface layers and dissolves in the Pd, leaving the surface clear for continued ethene

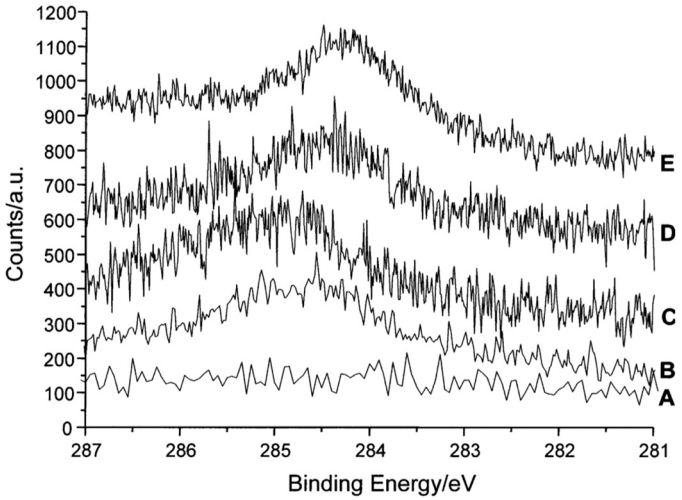

Fig. 5. XPS C(1 s) spectra before dosing ethene (lowest curve) and, from bottom to top, after ethene adsorption at 323 K, followed by heating to 373 and 473 K, together with the signal after adsorption at 423 K (top). Spectra C and D are multiplied by 3 compared with the others and each spectrum is offset vertically for clarity. From Bowker et al. [33].

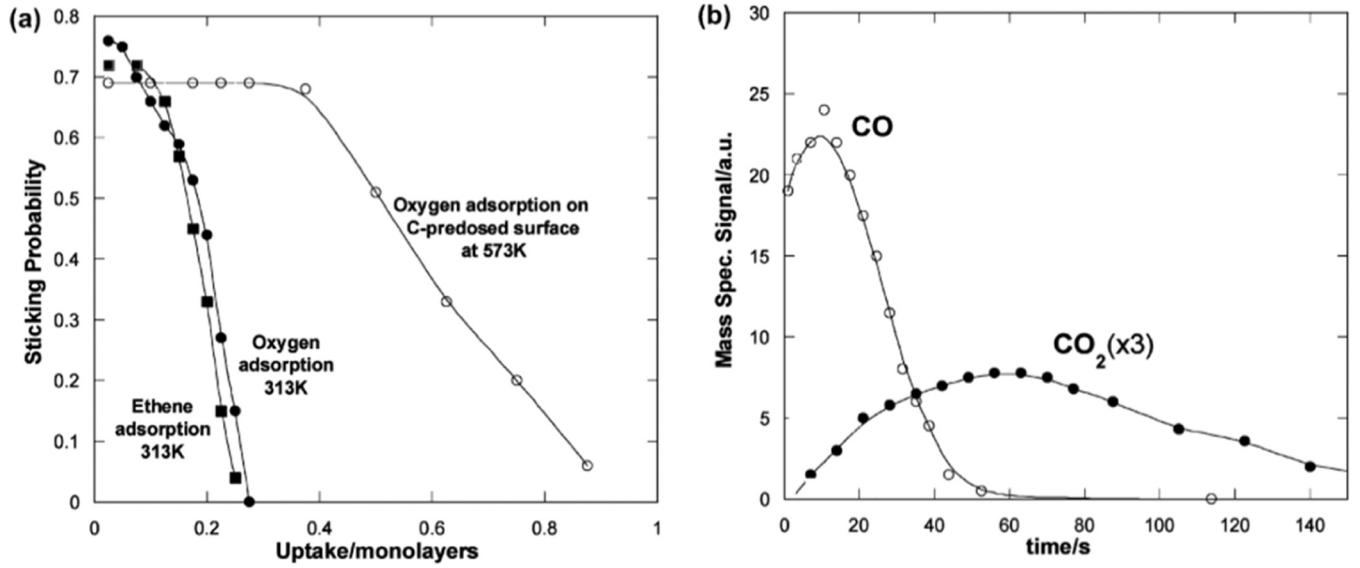

Fig. 4. a) shows the adsorption of ethene and oxygen on pure Pd(110) using the molecular beam reactor. The adsorption and uptake of both oxygen and ethene are very similar at low temperature on the clean surface. Note that the oxygen sticking and uptake on the clean surface is very similar even at 573 K. However, the high temperature oxygen result here is on the surface pre-treated with ethene at 573 K for 3 mins. During this adsorption products evolve into the gas phase (b) producing CO and CO_2 until all the adsorbed C is removed from the sample. From Bowker et al.3 [4].

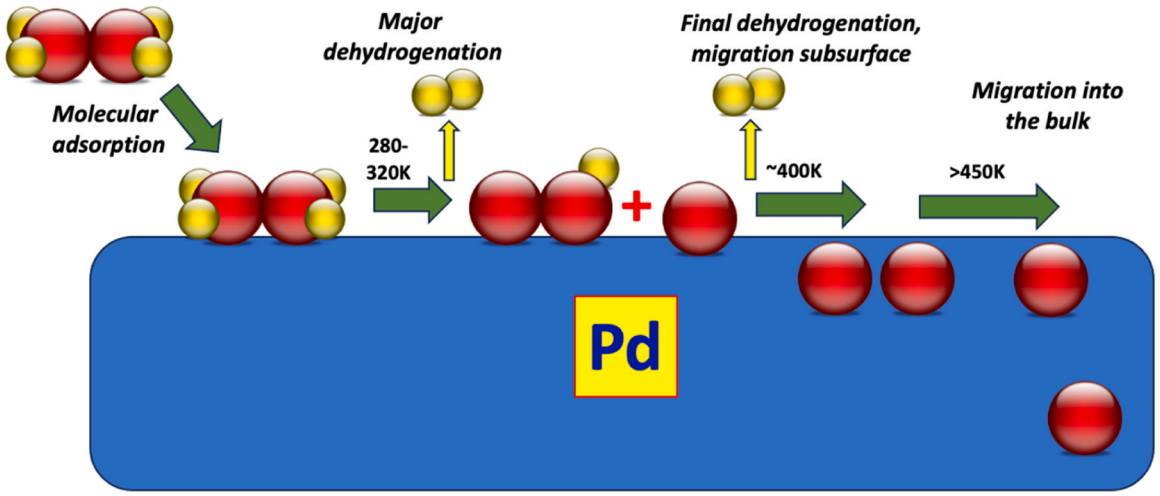

Fig. 6. A model for the reaction of ethene with bulk Pd, showing dehydrogenation to form surface carbon followed at higher temperatures by diffusion into the subsurface and into the bulk of the material. Adapted from Bowker et al. [33].

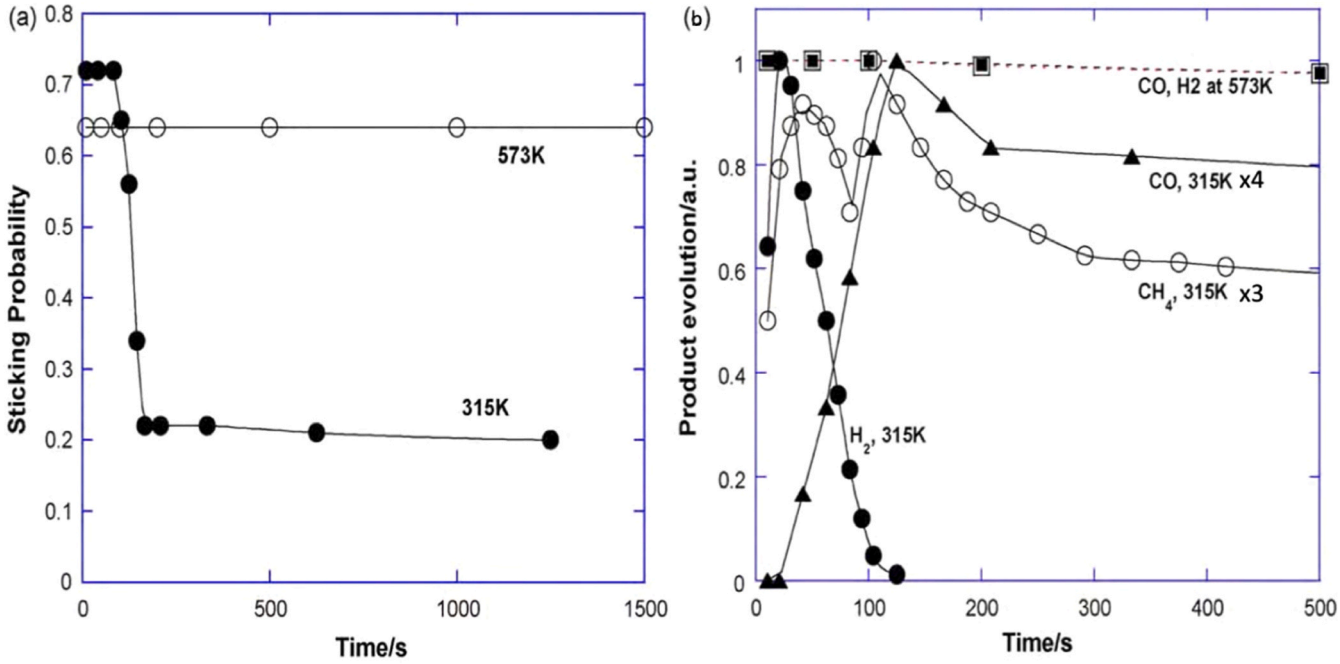

Fig. 7. a) The adsorption of acetaldehyde on Pd(110), showing high reactivity at 315 K, which drops to a lower steady state reactivity after ~ 100 s; at 573 K the reaction proceeds at a high steady state level immediately. b) corresponding with a) but showing product evolution at the two temperatures and showing decarbonylation at low temperature and dehydrogenation at higher temperature. Adapted from Bowker et al. [50].

adsorption and dissociation. If adsorption is carried out at an intermediate temperature, then the diffusion rate of the C into the surface becomes more limited and C tends to build up in the near-surface region and eventually reduces the adsorption rate because of C build up on the topmost surface layer itself [28,29].

The presence of C in the subsurface region is confirmed by subsequently exposing the surface to oxygen after removal of ethene from the gas phase. First CO evolves (when the surface oxygen level is low) and then CO_2 (when the surface oxygen is high) until the surface is clean of C again, and much more oxygen is adsorbed than is the case for the clean surface, Fig. 4 [29,30], due to the extra oxygen needed to react with the carbon. It is also seen by XPS, Fig. 5, where a carbidic-like material can be seen after heating (binding energy ~284.2 eV). Although this has a binding energy rather higher from the classic carbides which range from ~ 282–283.6 eV [44], it is also closer to Ni carbide [45] (at ~ 283.5 eV) and lower than that for the species left at ambient temperature after adsorbing ethene or surface carbon (~ 285 eV). The fact that it forms some kind of carbide at all goes against much opinion which indicates that it is unlikely. Thus, Jansson and Lewin suggest that Pd carbide forms only under "extreme conditions", whereas the conditions used here are far from extreme (moderate temperatures and very low pressures). [46]

As a result of these findings, and combined with data from XPS analysis of carbon loss from the surface region during moderate heating, a model for the processes involved is illustrated in Fig. 6. Here ethene adsorbs molecularly at low temperature and starts to dehydrogenate near ambient temperature to give hydrogen in the gas phase and adsorbed intermediates, which, depending on exact temperature may be a mix of C_2H and C on the surface. Above this further dehydrogenation of this mix takes place, especially above 400 K (Fig. 2), to leave C on the

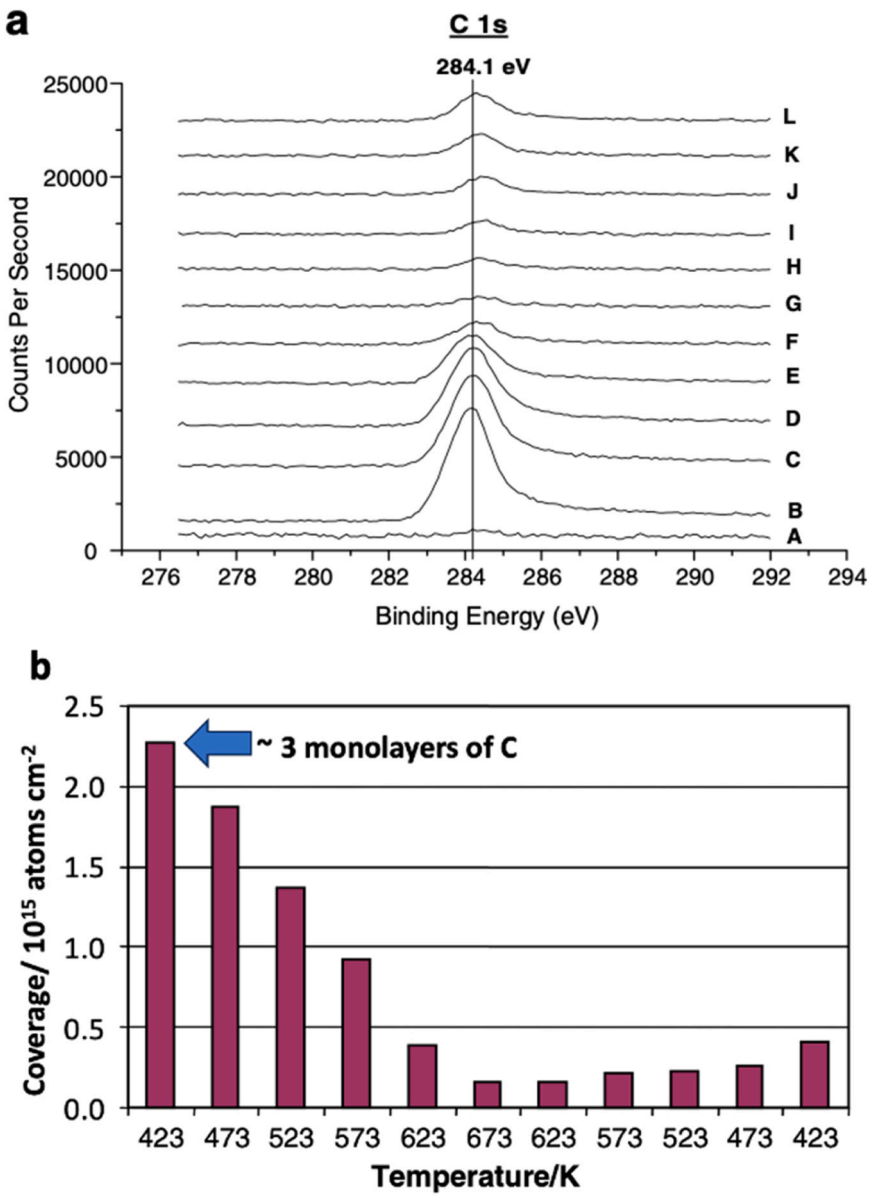

Fig. 8. a) X-ray photoelectron spectra for the C(1 s) region of the Pd(110) crystal showing A) the clean surface; B) after dosing acetaldehyde at 423 K;C) after heating to 473 K and subsequently after further heating in 50 K intervals (D, E, F), finally at 673 K (G). After this the sample is finally cooled again in 50 K intervals (I-K) finally reaching 423 K again (L). b) shows the estimates of coverage from the XPS during these temperature changes. Adapted from Bowker et al. [50].

surface which can migrate into the near-surface subsurface region. With further heating these species become even more mobile and can diffuse into the deep bulk of the material.

Such carbon deposition is not unique to ethene, other molecules such as alcohols [47–49], aldehydes [49–51], acids [52,53], enols and enals [49] will also react with the surface, decompose, and leave carbon behind. An interesting example of this is acetaldehyde [49]. Fig. 7 compares and contrasts the adsorption on Pd(110) at two different temperatures. At 315 K, there is an initial dehydrogenation of the molecule, which is short-lived and is followed by steady state decarbonylation of the molecule to CH_4 and CO, with an adsorption probability for the aldehyde of 0.2. What is happening here is that there is C-C scission initially, which results in CO and CH_3 deposition on the surface, with decomposition of the latter to give hydrogen in the gas phase and C on the surface. Once these have reached a certain coverage the dehydrogenation of the CH_3 group becomes very slow, such that it can be hydrogenated, and the CO has reached such a coverage that it is destabilised and desorbs. It is well known that the desorption profile of CO changes significantly with increasing coverage, shifting to lower temperatures [54–56]. When the reaction is carried out at 573 K the behaviour is different. Adsorption has a steady state value from the start, with a probability of 0.67, but now the CH_3 group is unstable, so the only gas phase products are H_2 and CO, leaving the C species on the surface. Again, as for ethene, though it might be expected that adsorption would stop as C builds up, it does not because the C diffuses subsurface at higher temperatures.

Similarly high sticking and C deposition is seen for other molecules such as acetic acid, vinyl acetate, higher alcohols and aldehydes.

The evidence that the C goes subsurface in these experiments at the higher temperatures is –

i) many layers equivalent of C can be adsorbed and yet adsorption does not stop;
ii) the C build-up under the surface can be removed with oxygen treatment;

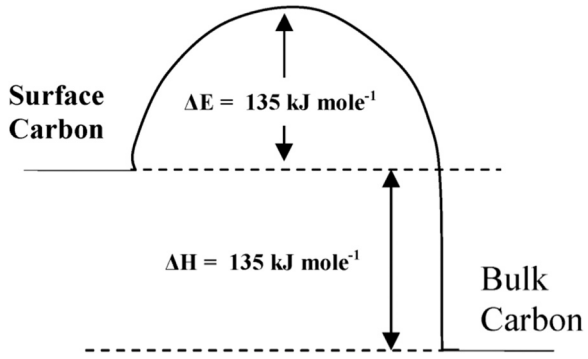

Fig. 9. Energetics of C dissolution and segregation back to the surface of Pd (110). [34].

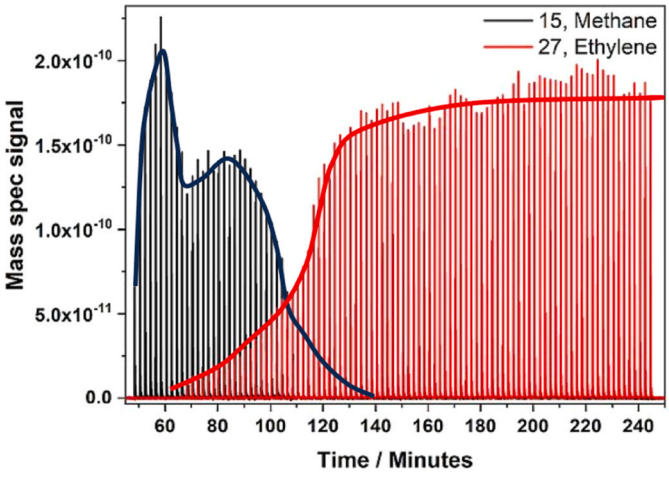

Fig. 10. The reaction of pulses of ethene with a 5 %Pd/SiO_2 catalyst at 573 K, showing disproportionation to CH_4 and leaving C on the catalyst. [35].

iii) XPS shows a carbide-like species after high temperature treatment (see Fig. 8 below);
iv) It is seen for nanoparticulate catalysts by XRD and XAS, as reported below.

Fig. 8 shows that, after adsorbing acetaldehyde on the Pd crystal surface at 423 K, there is significant coverage there, much more than a monolayer equivalent. At this temperature the molecule has decomposed to CO and hydrogen in the gas phase leaving the decomposed CH3 fragment behind as C. When this is heated it is lost from the surface region, and when it is cooled again it returns to the surface, but in a much more limited amount. In fact, by carefully measuring the effects of dosing amount and temperature on the amount of C deposited and that present at the surface (by oxygen clean-off measurements), and by modelling the processes, the energetics of the C interaction were estimated, as shown below (Fig. 9). [34] The estimated barrier for surface carbon to enter the bulk was approximately 135 kJ/mol and there is a similar value for the enthalpy of mixing into the bulk, which is exothermic. The latter was determined by low temperature clean-off of carbon appearing at the surface after kinetic measurements of annealing the sample for different times at varying isothermal temperatures above 750 K to get carbon to reappear at the surface, and thereby to determine the activation barrier to segregation. The enthalpy of mixing was determined by the temperature dependence of bulk to surface and surface to bulk activation energies and gives the exothermic heat of solution due to a very high barrier to segregation of ~270 kJ/mol, and hence the need to determine this at above 750 K. The barrier for C to get into the bulk is easier and begins above 400 K or so. The uncertainty in the barriers in these measurements is such that the enthalpy was estimated to be ~ ± 60 kJ/mol. Nevertheless, it is highly endothermic and even more energy-demanding to get C back to the surface layer.

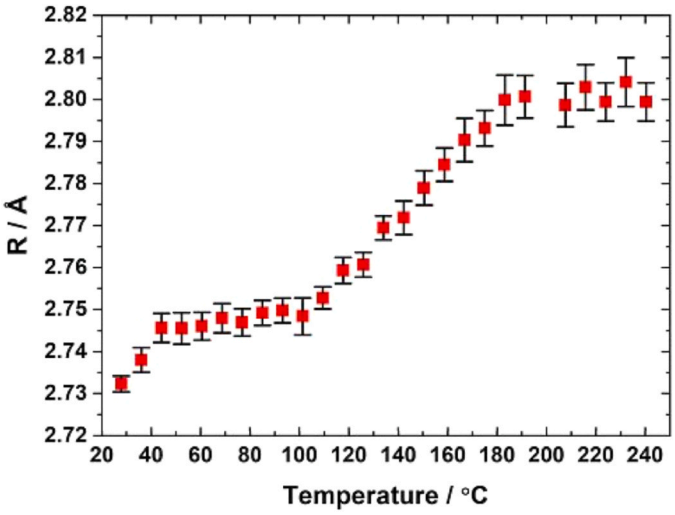

Fig. 11. Temperature programmed XAS taken in situ during exposure of a 4.4 wt% loading of Pd/SiO_2 to ethene and showing the lattice expansion due to carbide formation [35].

2.2. *Carbidisation of supported Pd catalysts*

When the reactivity of ethene is measured on supported nanoparticles in a reactor at ambient pressure [35], then the results are broadly similar in terms of C deposition. Thus Fig. 10 shows gas phase evolution during the reaction of Pd/SiO_2 with ethene at elevated temperature. After an initial short period when hydrogen is evolved and all ethene is adsorbed by the catalyst, no ethene leaves the end of the catalyst bed, but yet methane is evolved into the gas phase. After 10 pulses ethene begins to be seen at the end of the bed and reaction with the surface has stopped when the ethene reaches its saturation gas phase value after about 50 pulses. The disproportionation reaction which was occurring during this time is as follows –

$$C_2H_4 + Pd \rightarrow CH_4 + PdC_x$$

and reaction ceases when the bulk of the Pd is saturated with C. The presence of such C in the bulk was accompanied by a lattice expansion of ~ 2 % using XAS [35] (see Fig. 11) and XRD [35,57,58], and is also associated with some charge transfer from Pd to C [32]. The value of x in PdC_x was extimated to be ~ 0.25, by a combination of titration of the amounts of ethene reacted and the amount of CO_2 produced in subsequent oxygen clean-off experiments [32]. Note that this is somewhat higher than many claim (at ~ 0.17 [23,56,59,60]), but I consider that this is because the bulk of the Pd is saturated by carbidising at higher temperatures (up to 700 K) than is usually used by others. The fact that the ethene no longer is reactive with the surface after the bulk is saturated with carbon relates to the findings of Teischner et al. [23,25,26], who found that alkynes do not fully hydrogenate in the presence of hydrogen, and instead stop reacting at alkene formation when the surface is carbided.

3. Incorporation of other inorganics

Besides C incorporation described above, as with most metals Pd will oxidise into the bulk if exposed to oxygen at above 400 K, though Pt and Au are more resistant. Note that even Au can be oxidised under the right circumstances – for instance, if treated by oxygen atoms made by predissociation on a hot filament [61]

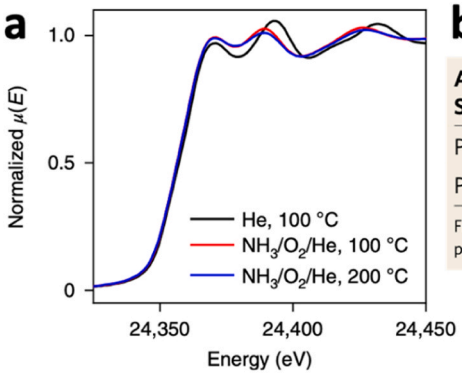

b

Absorber - Scatterer	N	R (Å)	σ^2 (Å^2)	E_0 (eV)	R_{factor}
Pd-N	1.0 (2)	2.00 (1)	0.003 (2)	−5.7 (4)	0.02
Pd-Pd	9.9 (1)	2.810 (5)	0.0161 (8)		

Fitting parameters: $S_0^2 = 0.8$; fit range $3 < k$ (Å^{-2}) < 10.6, $1 < R$ (Å) < 3; number of independent points = 9.

Fig. 12. a) Pd K-edge XANES spectra for 1.5 %Pd/γ-alumina showing changes when treated in NH_3-containing gases after pre-reduction in ammonia, showing changes associated with N incorporation onto the Pd. b) Fitted K-edge Pd EXAFS parameters for the sample treated at 100 °C in 0.5 %NH_3/2.5 %O_2/He. From Dann et al. [62].

However, there are also other inorganics that can interact with Pd and dissolve into the bulk, and one of these is nitrogen. Dann et al. [62] have recently shown that N can be incorporated into the Pd lattice during ammonia oxidation catalysis (Fig. 12) resulting in an expansion of the Pd lattice of a similar value to that for C insertion above. Here the effect of bulk and surface N is important because it directs the selectivity of ammonia oxidation towards N_2 production, rather than towards N_2O.

McCue et al. [63] prepared Pd_4S (note the similar stoichiometry to $PdC_{0.25}$ above) by careful reduction of $PdSO_4$ and showed this material to have excellent stability and selectivity in partial alkyne hydrogenation to the alkene. Ma et al. [64] prepared supported Pd_4S materials in a different way by careful sulphidation of Pd in H_2S/H_2 mixtures. These materials also showed good stability and activity, but this time for methane total oxidation.

4. Conclusions

Pd shows a facile ability to absorb other inorganic atoms into its bulk and here the focus is on carbon incorporation into the Pd lattice. In this review I have shown that this occurs when it is exposed to a range of organic molecules, including alkenes, alcohols, aldehydes, acids and a range of other species, and begins to occur above around 400 K. In particular, when treated in ethene, dehydrogenation occurs on bulk Pd samples, putting C into the bulk, while with nanoparticulate Pd, the bulk of the particle can become quickly saturated with carbon. This occurs through a disproportionation reaction in which methane is a co-product. This then results in reduced reactivity for dehydrogenation of the nanoparticles, and probably relates to important industrial reactions such as acetylene hydrogenation, where over-hydrogenation needs to be avoided to result in high selectivity for partial hydrogenation to ethene.

CRediT authorship contribution statement

M. Bowker: Writing – review & editing, Writing – original draft, Supervision, Resources, Project administration, Methodology, Investigation, Funding acquisition, Formal analysis, Data curation, Conceptualization.

Declaration of Competing Interest

The author declares no conflict of interest.

Data Availability

Data will be made available on request.

Acknowledgements

I thank the Max Planck Society and Cardiff University for financial support to create the FUNCAT Centre. I also thank the UK Catalysis Hub, funded through EPSRC Grants EP/R026939/1 and EP/R026815/1, and from EPSRC EP/ S030468/1, EP/ N010531/1.

References

[1] A. Balandin, Adv. Catal. 19 (1969) 1–210, 1969.
[2] P. Sabatier, Ber Dtsch, Chem. Ges. 44 (1911) 1984–2001.
[3] G.C. Bond, Heterogeneous Catalysis, Oxford University Press, Oxford, 1987, pp. 62–69.
[4] "Catalysis", ch 3, p 83 (eds J.A. Moulijn, P. van Leeuwen and R. A. van Santen) NIOK 1993.
[5] "Chemical Kinetics and Catalysis" R. A. van Santen and J. W. Niemantsverdriet, ch 6 (1995, Plenum, New York).
[6] M. Bowker, The Basis and Applications of Heterogeneous Catalysis, Oxford University Press, 1998, pp. 51–52.
[7] J. M, J.W. Thomas, Principles and Practice of Heterogeneous Catalysis, VCH, Weinheim, 1997, p. 29.
[8] C.J.H. Jacobsen, S. Dahl, B.S. Clausen, S. Bahn, A. Logadottir, K. Jens, Nørskov, J. Am. Chem. Soc. 123 (2001) 8404–8405.
[9] A. Daisley, J.S.J. Hargreaves, R. Hermann, Y. Poya, Y. Wang, Catal. Today 357 (2020) 534–540.
[10] M.R. Rahimpour, M. Jafari, D. Iranshahi, Appl. Energy 109 (2013) 79–93.
[11] O. Lopez, J.M. Padron, Catalysts 12 (2022) 164.
[12] R. Guil-Lopez, et al., Materials 12 (2019) 3902.
[13] V. Shadravan, et al., Energy Environ. Sci 15 (2022) 3310.
[14] J.R. Jennings and S.A. Ward, Ammonia Synthesis, in Catalyst Handbook, 2nd edition, ed. M. Twigg (Wolfe, Frome, England, 1989) pp 395-398.
[15] D. Vandervell, K.C. Waugh, Chem. Phys. Letters 171 (1990) 462–468.
[16] V.A. Mazzieri, J.M. Grau, C.R. Vera, J.C. Yori, J.M. Parera, C.L. Pieck, Catal. Today 107-108 (2005) 643–650.
[17] J. Nakamura, I. Nakamura, T. Uchijima, Y. Kanai, T. Watanabe, M. Saito, T. Fujitani, Catal. Lett. 31 (1995) 325.
[18] S. Kattel, P.J. Ramírez, J.G. Chen, J.A. Rodriguez, P. Liu, Science 355 (2017) 1296–1299.
[19] M. Behrens, F. Studt, I. Kasatkin, S. Kühl, M. Hävecker, F. Abild-Pedersen, S. Zander, F. Girgsdies, P. Kurr, B.-L. Kniep, M. Tovar, R.W. Fischer, J.K. Nørskov, R. Schlögl, Science 336 (2012) 893–897.
[20] M.S. Spencer, Top. Catal. 8 (1999) 259–266.
[21] S.J. Thomson, G. Webb, J. Chem. Soc. (1976) 526–527.
[22] G. Webb, Catal. Today 7 (1990) 139–155.
[23] D. Teschner, et al., J. Catal. 242 (2006) 26–37.
[24] R. Kennedy, G. Webb, S.D. Jackson, D. Lennon, Appl. Cat. A. 259 (2004) 109–120.
[25] D. Teschner, J. Borsodi, A. Wootsch, Z. Révay, M. Hävecker, A. Knop-Gericke, S.D. Jackson, R. Schlögl, 320 (2008) 86.
[26] D. Teschner, et al., Angew. Chem. 120 (2008) 9414–9418.
[27] A.M. Alexander, J.S.J. Hargreaves, Chem. Soc. Rev., 39 (11), 4388-4401.
[28] M. Bowker, T. Aslam, C. Morgan, N. Perkins, in: S.D. Jackson, J. Hargreaves, D. Lennon (Eds.), 'Catalysis in Application', RSC, Cambridge, 2003, pp. p1–p7.
[29] M. Bowker, C. Morgan, J. Couves, Surf. Sci. 555 (2004) 145–156.
[30] M. Bowker, C. Morgan, Cat. Letters 98 (2004) 67.
[31] M. Bowker, C. Morgan, V. Zhdanov, PCCP 9 (2007) 5700.
[32] C. Morgan, M. Bowker, Surf. Sci. 603 (2009) 54–59.
[33] M. Bowker, C. Morgan, N. Perkins, R. Holroyd, E. Fourre, F. Grillo, A. MacDowall, J. Phys. Chem. B 109 (2005) 2377–2386.
[34] M. Bowker, J. Counsell, K. El-Abiary, L. Gilbert, C. Morgan,S. Nagarajan, C. S. Gopinath, J. Phys. Chem. C. 114 (2010) 5060–5067.

[35] W. Jones, P.P. Wells, E.K. Gibson, A. Chutia, I.P. Silverwood, C.R.A. Catlow, M. Bowker, Chem. Cat. Chem. 11 (2019) 4334–4339.
[36] A.L. Bugaev, O.A. Usoltsev, A. Lazzarini, K.A. Lomachenko, A.A. Guda, R. Pellegrini, M. Carosso, J.G. Vitillo, E. Groppo, J.A. van Bokhoven, A.V. Soldatov, C. Lamberti, Faraday Discuss.. 208 (2018) 187–205.
[37] A.L. Bugaev, Alexander A. Guda, I.A. Pankina, E. Groppo, R. Pellegrini, A. Longod, A.V. Soldatov, C. Lamberti, Catal. Today *336* (2019) *40–44*.
[38] A.A. Skorynina, A.A. Tereshchenko, O.A. Usoltsev, A.L. Bugaev, K.A. Lomachenko, A.A. Guda, E. Groppo, R. Pellegrini, C. Lamberti, A.V. Soldatov, Radiat. Phys. Chem. *175* (2020) 108079.
[39] O.A. Usoltsev, A.Y. Pnevskaya, E.G. Kamyshova, A.A. Tereshchenko, A. A. Skorynina, Z. Wei, T. Yao, A.L. Bugaev, A.V. Soldatov, Nanomaterials 10 (2020) 1643.
[40] Y. He, C. Wu, J. Phys. Chem. C. 125 (2021) 20930–20939.
[41] A. Kordatos, K. Mohammed, R. Vakili, A. Goguet, H. Manyar, E. Gibson, C. M. Carravetta, P. Wells, C.-K. Skylaris, RSC Adv. 13 (2023) 5619–5626.
[42] M. Nishijima, J. Yoshinobu, T. Sekitani, M. Onchi, M. J. Chem. Phys. 90 (1989) 5114.
[43] T. Sekitani, T. Takaoka, M. Fujisawa, M. Nishijima, J. Phys. Chem.. 96 (1992) 8462.
[44] G. Greczynski, D. Primetzhofer, L. Hultman, Appl. Surf. Sci. 436 (2018) 102–110.
[45] A. Furlan, J. Lu, L. Hultman, U. Jansson, M. Magnuson, J. Phys.: Condens. Matter 26 (2014) 415501.
[46] U. Jansson, E. Lewin, Thin Solid Films 536 (2013) 1–24.
[47] R. Holroyd, M. Bowker, Surf. Sci. 377- 379 (1997) 786–790.
[48] S. Francis, J. Corneille, D.W. Goodman, M. Bowker, Surf. Sci. 364 (1996) 30–38.
[49] M. Bowker, R. Holroyd, N. Perkins, L. Gilbert, J. Counsell, C. Morgan, J. Phys. Chem. C. 114 (2010) 17142–17147.
[50] M. Bowker, Richard Holroyd, Neil Perkins, Jenita Bhantoo, Jonathon Counsell Albert Carley, Chris Morgan, Surf. Sci. 601 (2007) 3651–3660.
[51] M. Bowker, L. Cookson, J. Bhantoo, A. Carley, E. Hayden, L. Gilbert, C. Morgan, J. Counsell, Appl. Catal. A: Gen. 391 (2011) 394–399.
[52] M. Bowker, C. Morgan, J. Couves, Surf. Sci. 555 (2004) 145–156.
[53] M. Bowker, C. Morgan, V. Zhdanov, PCCP 9 (2007) 5700.
[54] I. Jones, R. Bennett, M. Bowker, Surf. Sci. 439 (1999) 235–248.
[55] K. Yagi-Watanabe, H. Fukutani, J. Chem. Phys. 112 (2000) 7652–7659.
[56] H. Conrad, G. Ertl, J. Koch, E.E. Latta, Surf. Sci. 43 (1974) 264–280.
[57] S.B. Ziemecki, G.A. Jones, D.G. Swartzfager, R.L. Harlow, J. Am. Chem. Soc. 107 (1985) 4547–4548.
[58] O. Balmes, et al., Phys. Chem. Chem. Phys. 14 (2012) 4796–4801.
[59] J.A. McCaulley, J.Phys Chem *97* (1993) 10372–10379.
[60] M.A. Newton, M. Di Michiel, A. Kubacka, A. Iglesias-Juez, M. Fernandez-García, Angew. Chem. Int. Ed. 51 (2012) 2363–2367.
[61] G. Sault, R.J. Madix, C.T. Campbell, Surf. Sci. 169 (1986) 347–356.
[62] E.K. Dann, et al., Nat. Catal. 2 (2019) 157–163.
[63] A.J. McCue, A. Guerrero-Ruiz, I. Rodríguez-Ramos, James A. Anderson, J. Catal. 340 (2016) 10–16.
[64] L. Ma, S. Yuan, H. Zhu, T. Jiang, X. Zhu, C. Lu, X. Li, Catalysts 9 (2019) 410.